

# Zooming in: High Resolution 3D Reconstruction of Differently Stained Histological Whole Slide Images

Johannes Lotz<sup>\*1</sup>, Judith Berger<sup>\*1</sup>, Benedikt Müller<sup>3</sup>, Kai Breuhahn<sup>3</sup>, Niels Grabe<sup>4</sup>, Stefan Heldmann<sup>1</sup>, André Homeyer<sup>2</sup>, Bernd Lahrmann<sup>3,4</sup>, Hendrik Laue<sup>2</sup>, Janine Olesch<sup>1</sup>, Michael Schwier<sup>2</sup>, Oliver Sedlaczek<sup>5</sup>, Arne Warth<sup>3</sup>

<sup>1</sup>Fraunhofer MEVIS, Project Group Image Registration, Lübeck, Germany; <sup>2</sup>Fraunhofer MEVIS, Bremen, Germany; <sup>3</sup>Institute of Pathology, University Hospital Heidelberg, Germany; <sup>4</sup>Tissue Imaging and Analysis Center, University of Heidelberg, Germany; <sup>5</sup>Radiologische Klinik, University Hospital Heidelberg, Germany

## 1. ABSTRACT

Much insight into metabolic interactions, tissue growth, and tissue organization can be gained by analyzing differently stained histological serial sections. One opportunity unavailable to classic histology is three-dimensional (3D) examination and computer aided analysis of tissue samples. In this case, registration is needed to reestablish spatial correspondence between adjacent slides that is lost during the sectioning process. Furthermore, the sectioning introduces various distortions like cuts, folding, tearing, and local deformations to the tissue, which need to be corrected in order to exploit the additional information arising from the analysis of neighboring slide images.

In this paper we present a novel image registration based method for reconstructing a 3D tissue block implementing a zooming strategy around a user-defined point of interest. We efficiently align consecutive slides at increasingly fine resolution up to cell level. We use a two-step approach, where after a macroscopic, coarse alignment of the slides as preprocessing, a nonlinear, elastic registration is performed to correct local, non-uniform deformations. Being driven by the optimization of the normalized gradient field (NGF) distance measure, our method is suitable for differently stained and thus multi-modal slides.

We applied our method to ultra thin serial sections (2  $\mu\text{m}$ ) of a human lung tumor. In total 170 slides, stained alternately with four different stains, have been registered. Thorough visual inspection of virtual cuts through the reconstructed block perpendicular to the cutting plane shows accurate alignment of vessels and other tissue structures. This observation is confirmed by a quantitative analysis. Using nonlinear image registration, our method is able to correct locally varying deformations in tissue structures and exceeds the limitations of globally linear transformations.

## 2. DESCRIPTION OF PURPOSE

In cancer diagnostics and histology-related basic research, much insight into metabolic interactions, tissue growth, and tissue organization can be gained by analyzing differently stained histological serial sections. For this procedure, a fixed tissue block is cut into ultra thin slides which are then examined by microscopy. An inevitable downside of the histological sectioning is the loss of spacial correspondence between adjacent slides. For this reason, also the 3D information is completely missing although it is valuable, for example for pathologists and biologists analyzing vascular structure or tumor dissemination[1]. Furthermore, the cutting process introduces various distortions like cuts, folding, tearing, or local elastic distortions to the tissue. For a high resolution reconstruction of a block and slide-to-slide comparison up to cell-level, especially elastic distortions of the tissue need to be corrected. Large cuts, folds and tearing can often not be undone and will not be addressed here. However, smaller of these artifacts need to be handled robustly in order to be able to register the tissue in their vicinity.

In non-digital histological studies, the combination of different staining chemicals on one slide is necessary but often difficult due to their mutual reactions. Using different stains on consecutive ultra thin slides, a multi-modal registration method allows for a virtual double staining of the tissue. Furthermore, additional information can be gained by the visualization and analysis of the three dimensional structure of the tissue. In a recent publication [1, 2] the authors report that

---

\* corresponding authors, E-Mail: {lotz,berger}@mevis.fraunhofer.de

3D reconstruction enables the automatic detection of tumor islands in lung adenocarcinomas. The authors use the detected tumor islands as a diagnostic criterion and show a significant decrease in survival rate in patients where tumor islands are found. In their study, more than 260 histological datasets are manually reconstructed.

Automatic registration in histological imaging and digital pathology in general is an upcoming topic of research. A few methods have been proposed aiming at automatic 3D reconstructions including [3], [4], and [5] to name just a few. Especially in histology, images are usually available in a very high image resolution resulting in images with more than  $10^{10}$  pixels. Some approaches dealing with the large size of histological images will be briefly sketched here.

In [6], the authors describe an algorithm that performs a three dimensional tissue reconstruction of histological sections that are differently stained. The authors propose a tile based approach previously published by [7] that first computes a rough globally rigid transformation which is then refined by calculating rigid transformations on smaller tiles of the image with higher resolution. Multi-modal registration between differently stained sections is achieved by an automated content classification. A global nonlinear deformation is computed by interpolating between rigidly transformed points on individual tiles using b-spline transformations. These methods require manual correction in case of failure in the initial rigid registration. Another way to find correspondences is to detect image features such as blood cells or vessels. In [8] a tile based approach is combined with SIFT feature detection whereas in [9] red blood cells are identified in mono-modal images.

### 3. METHOD

We propose a tile-based method but calculate an elastic deformation instead of affine or rigid transformations. Our method is fully automatic and does not involve human intervention once the target area has been selected initially. Multi-modality is dealt with by a flexible distance measure that evaluates similarity of two images based on edges instead of finding point correspondences or using machine learning approaches.

We consider a given a series of consecutive histological images  $I_1, \dots, I_n$  defined on image domains  $\Omega_1, \dots, \Omega_n$  and assume that the images are stained in alternating order. The central component of our reconstruction scheme is the registration of two consecutive images. Since these images are almost certainly not of the same staining, we assume this registration problem to be multi-modal. Registering two slide images  $I_j$  and  $I_{j+1}$  we start with a parametric, affine registration based on a coarse-to-fine scheme. Once this correspondence is established, we continue to zoom in around a user defined point of interest as seen in [10].

While zooming in in terms of increasing the magnification level, we keep the resolution of the chosen image section constant at  $2048 \times 2048$  pixels. The tile size can be determined by the user and is a compromise between visible tissue area and processing time. The zooming step is repeated until the desired image resolution is reached, resulting in two affinely registered high resolution tiles from two adjacent whole slide images. See Figure 1 for an illustration of the complete registration scheme.

To cope with the multi-modality of the images, we choose the NGF [11] distance measure with

$$\mathcal{NGF}[I_j, I_{j+1}, y_j] = \int_{\Omega_j} 1 - \frac{\nabla I_{j+1}(y_j(x))^T \nabla I_j(x) + \eta^2}{\sqrt{\|\nabla I_{j+1}(y_j(x))\|_2^2 + \eta} \sqrt{\|\nabla I_j(x)\|_2^2 + \eta}} dx. \quad (1)$$

which is numerically optimized with respect to a deformation  $y_j : \Omega_j \rightarrow \Omega_{j+1}$  that describes the correspondence between adjacent slides. Using NGF, the distance of two images is expressed by evaluating the alignment of their edges instead of focussing on absolute pixel values. Due to the normalization term in the denominator, a pure implementation of a normalized gradient with  $\eta = 0$  would treat all edges in the image equally. The edge coefficient  $\eta$  acts as a noise filter by reducing the influence of those image gradients  $\nabla I(x)$  that are significantly smaller than  $\eta$ .

NGF not only allows the registration of differently stained images but also copes nicely with different staining intensities in same-stain (mono-modal) registration. Though a purely affine model ensures a robust and regular deformation also in the presence of small artifacts, it does not account for nonlinear distortions.

For further refinement we apply a nonlinear registration to the high resolution image block, minimizing a functional that combines the NGF distance measure and a regularizer  $\mathcal{S}$  with respect to the displacement  $y_j$ :

$$\mathcal{J}[I_j, I_{j+1}, y_j] = \mathcal{NGF}[I_j, I_{j+1}, y_j] + \mathcal{S}[y_j] \xrightarrow{y_j} \min. \quad (2)$$

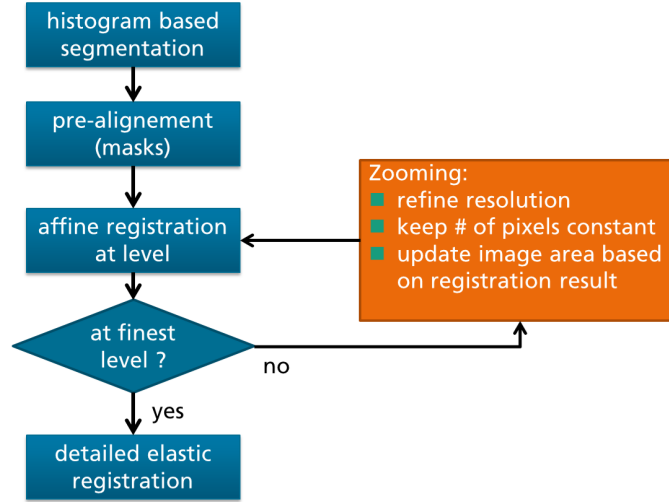


Figure 1. Flowchart of the implemented registration scheme. After a coarse segmentation based pre-alignment, first affine and consecutively elastic registration is performed.

The regularizer is used to define the deformation model assumed in the registration and to ensure smoothness and robustness. As the local deformations in the slides stem from the sectioning process where the tissue is expected to behave mostly elastic, we use the elastic regularizer

$$\mathcal{S}[y_j] = \alpha \frac{1}{2} \int_{\Omega} \mu \langle \nabla y_j(x), \nabla y_j(x) \rangle + (\lambda + \mu) (\nabla \cdot y_j(x))^2 dx. \quad (3)$$

In order to optimize the joint objective function  $\mathcal{J}[I_j, I_{j+1}, y_j]$ , a Gauss-Newton scheme is applied using discretized analytic derivatives [12].

The 3D reconstruction is computed by a consecutive parametric (affine) registration of neighboring slides which is refined by applying a nonlinear (elastic) registration to the affinely pre-registered stack. Using the first slide  $I_1$  as reference, all consecutive slides are registered according to the original cutting sequence independently of staining. This order proved to be successful in a comparison of different slide registration approaches [6]. In order to examine the 3D structure at cell level which is more important from a clinical perspective, we use the zooming strategy to reconstruct an isolated block of tissue at high resolution. The position of the reconstructed block can be chosen freely in the dataset.

## 4. RESULTS

In order to evaluate our algorithm on clinically relevant samples, we applied the reconstruction method to a stack of 202 slides of human lung tumor [13] (non-small cell lung cancer, NSCLC) generated within the LungSys2 consortium\*. The surgically resected material was fixed, sectioned with a slice thickness of  $2 \mu m$ , and immunohistochemically stained alternately with four different stains (CD31, H&E, factor VIII, KL-1). The images  $\{I_j | j = 4z + k, z = 0, \dots, 49\}$  are stained with CD31 for  $k = 1$ , H&E for  $k = 2$ , factor VIII for  $k = 3$  and KL-1 for  $k = 4$ . The sections were digitized and converted into an in-house implemented format, making use of a coarse-to-fine multilevel image data structure based on an SQLite database. In total, 202 whole slide images are available at 40x (KL-1, factor VIII, CD31) or 20x (H&E) magnification. The zooming step was repeated until a pixel length of  $0.45 \mu m$  (level 1) was reached. We excluded 32 slides due to heavy scanning or staining artifacts or due to excessive tissue damage, resulting in 170 slides for the reconstruction.

We evaluated our registration qualitatively by visual inspection and quantitatively by measuring the alignment of manual annotations in the image.

The visual inspection of the registered slides was performed on virtual cuts through the reconstructed block which are shown in Figure 2. The checkerboard overlay of two consecutive slides shown in Figure 3 (left), illustrates precisely aligned

\*LungSys2 is funded by the German Ministry of Education and Research, see [www.lungSys.de](http://www.lungSys.de) for further information.

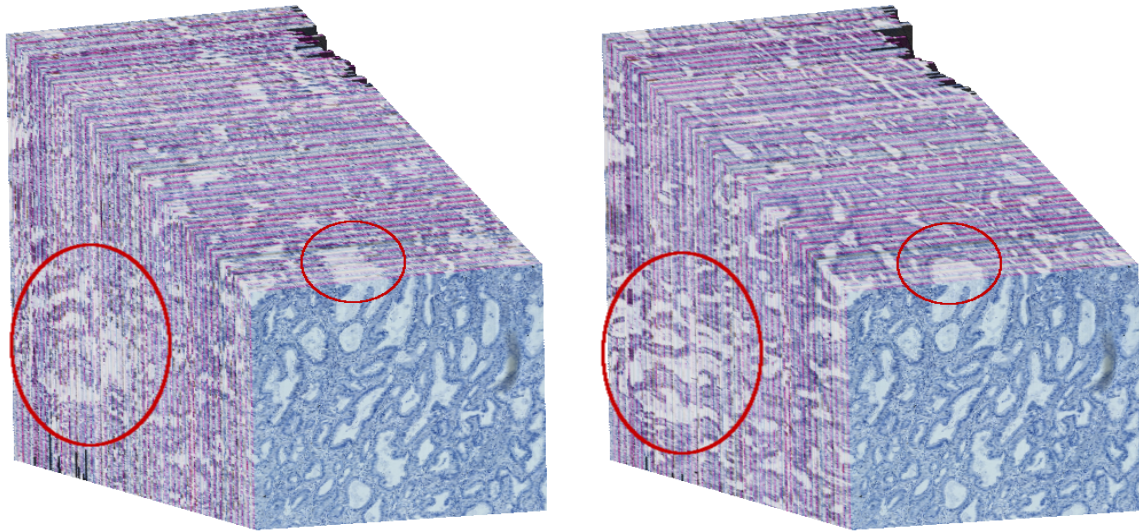


Figure 2. 3D reconstruction of the whole image stack (170 slides). Shown is an image section of size  $2048 \times 2048$  at 5x magnification, which is cropped by virtual clipping planes. LEFT: Reconstruction after affine registration, RIGHT: Reconstruction after elastic registration showing smoother appearance of anatomical structures.

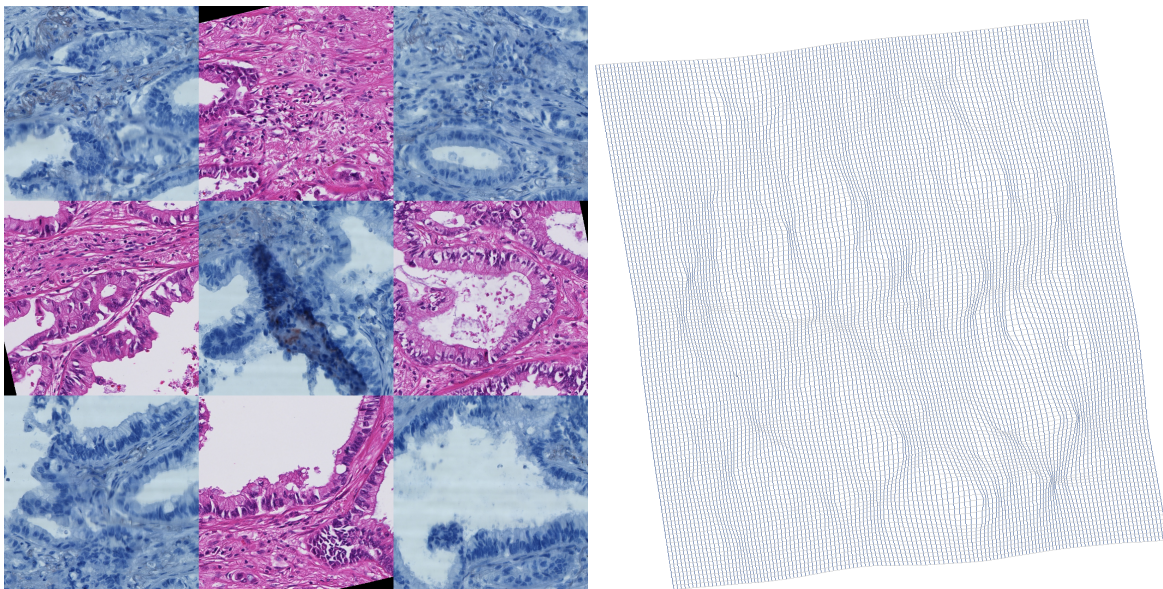


Figure 3. LEFT: 20x magnified checkerboard overlay of consecutive slides: CD31 stained slide with elastically registered (i.e. deformed) H&E stained neighboring slide. A staining artifact in the center of the blue CD31 image does not compromise the registration result. RIGHT: Calculated elastic deformation field.

structures after elastic registration. Comparing the 3D rendering of virtual cuts of an affine and an elastic reconstruction, Figure 2 shows vessels and anatomical structures that can be tracked very smoothly through the elastically registered tissue block, while being hardly noticeable after purely affine registration. The exemplary shown deformation field visualized in Figure 3 (right) shows both the smoothness of the calculated deformation and also the necessity for nonlinear modeling.

Mapping anatomically corresponding image features onto each other, the registration can be evaluated quantitatively by measuring the alignment of morphologically prominent image features. As the prominent structures in the images include mostly alveolas and vessels which are relatively round in shape, the manual placement of landmarks has shown to be unreliable and had to be discarded as an evaluation criterion. Instead, the borders of two structures were manually

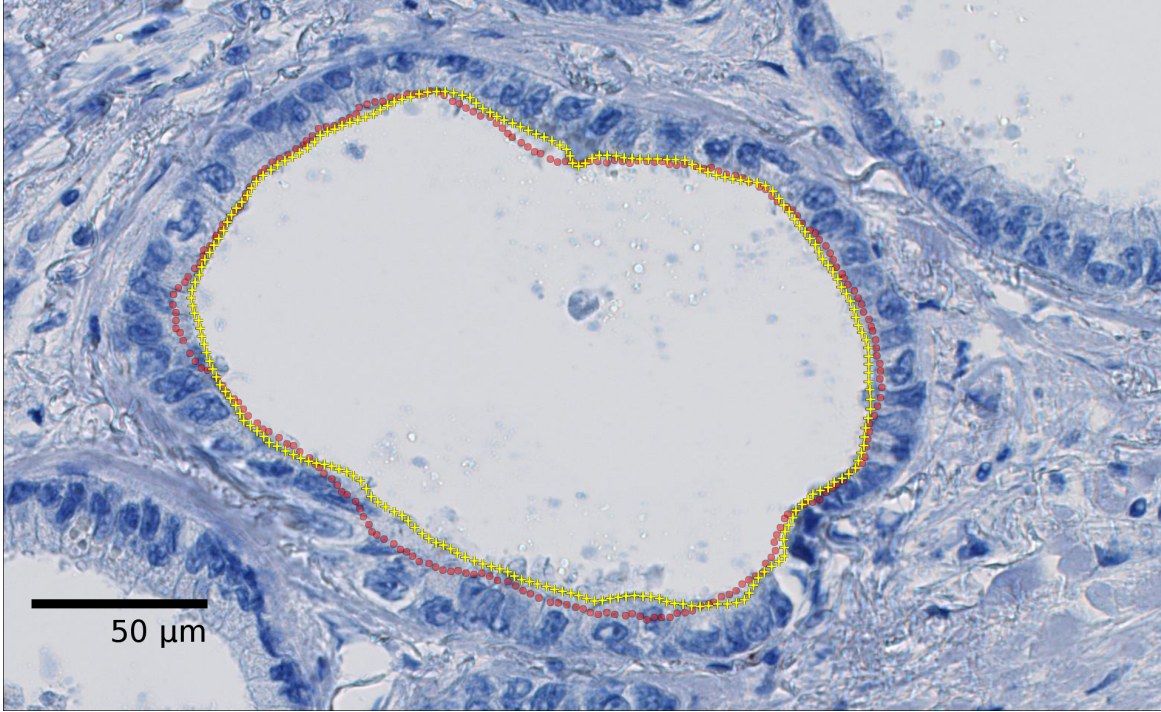


Figure 4. Roundly shaped structure in a factor VIII stained slide with annotation (yellow crosses). Superimposed is the annotation of the corresponding structure in the previous slide after being deformed by the nonlinear registration result (red dots).

segmented by a smoothed, closed freehand contour in four consecutive slides before registration. An example of such a segmentation is shown in Figure 4. The results of the linear registration at different zooming levels as well as the result of the nonlinear registration at the finest zooming level were applied to deform these segmentations for each pair of neighboring slides.

We choose the Hausdorff distance  $h_d$  of two segmentations represented by point sets  $A = \{a_1, \dots, a_N\}$  and  $B = \{b_1, \dots, b_M\}$  for example described in [14] with

$$h_d(A, B) = \max\left\{ \max_{a \in A} \min_{b \in B} \|a - b\|_2, \max_{b \in B} \min_{a \in A} \|b - a\|_2 \right\}$$

as error measure. Being intuitive in terms of absolute displacement error, the Hausdorff distance can be interpreted as the maximum error of the registration result on the (discretized) border of the annotated structure. This is a main advantage over relative measures such as the otherwise popular dice coefficient [15] which is relative to the annotated area and therefore unfit to compare results between different annotations or data sets.

The segmentations are represented by discrete point sets of an average distance of 3  $\mu\text{m}$  between adjacent points. For the first three slide pairs, the registration results were applied to these point sets in the reference image and compared to the unaltered point sets in the template image. The Hausdorff distance was computed on three levels (5, 3, and 1) after linear registration and after the final nonlinear registration (level 1). These measurements are shown in Table 1. The average distance in the annotated structures is 7.73  $\mu\text{m}$ . The measurements show the increase in accuracy after registration at higher magnification. The results also confirm the additional benefit of the nonlinear registration which lowers the calculated distance significantly (mean  $d_h$  is smaller after nonlinear registration than after finest level linear registration, one-sided t-test,  $p < 0.05$ ). An evaluation including a higher number of slides is currently in preparation.

The computed distances give a good impression of the registration accuracy but do not replace visual inspection. A perfect alignment of the annotations is neither possible nor desired. Due to the inaccuracies of manual annotations in tissue, a zero distance between the annotations is very unlikely, even if the registration was perfect. Furthermore, a registration

resolution level	registered slides	$d_h$ (structure a)	$d_h$ (structure b)
5 (affine)	1 → 2	8.95	37.94
3 (affine)	1 → 2	9.14	7.58
1 (affine)	1 → 2	8.61	7.76
1 (nonlinear)	1 → 2	<b>8.43</b>	<b>7.19</b>
5 (affine)	2 → 3	20.89	16.69
3 (affine)	2 → 3	7.60	10.80
1 (affine)	2 → 3	7.06	10.74
1 (nonlinear)	2 → 3	<b>6.04</b>	<b>8.97</b>
5 (affine)	3 → 4	14.06	24.56
3 (affine)	3 → 4	8.99	9.45
1 (affine)	3 → 4	8.80	9.31
1 (nonlinear)	3 → 4	<b>7.05</b>	<b>8.72</b>

Table 1. Alignment errors  $d_h$  of the annotations of two structures (a and b) after registration at different registration levels expressed in Hausdorff distance. Final results are highlighted in **bold**. Three slide pairs were annotated. Pixel length at level 1 is 0.45  $\mu\text{m}$ . Mean Hausdorff Distance after nonlinear registration: 7.73  $\mu\text{m}$ .

that perfectly maps the structures of two slides onto each other would destroy the 3D information encoded in the structural differences from slide to slide.

Before computationally processing the data, the tissue block undergoes the process of cutting, staining, counter-staining and scanning. This data acquisition part is by far more time consuming than the final digital 3D reconstruction. However, fast computation is an advantage, especially in the case of serial histologic sectioning where a high amount of data has to be processed. The time the presented algorithm needs to process one pair of slides up to 20x magnification (2048  $\times$  2048 pixels, 0.45  $\mu\text{m}$  pixel length) is approximately 40 seconds on a dual core laptop computer equipped with an Intel Core i7-3520M CPU at 2.9 GHz.

## 5. CONCLUSIONS

We presented a novel method for fast fully automatic high resolution 3D reconstruction of serial sections. The registration framework includes an affine pre-alignment based on the NGF distance measure including a zooming strategy. NGF provides the flexibility to register differently stained slide images which was shown on four different immunohistochemical stains. Finally local elastic distortions introduced to the tissue by the sectioning process are refined in a nonlinear step using an elastic registration model. After elastic refinement, virtual cuts through the reconstructed tissue block show smooth structures which were not visible in the affine reconstruction. The computed distances between annotated structures in the images show the high accuracy of the registration. The presented method allows an easy extension towards a reconstruction of the whole slide area at high resolutions of up to 20x or even 40x by combining the computed elastic deformations of neighboring tiles after zooming. Necessary modifications to data storage and handling are currently in preparation.

## References

- [1] Maristela L Onozato et al. "A role of three-dimensional (3D)-reconstruction in the classification of lung adenocarcinoma." In: *Analytical cellular pathology (Amsterdam)* 35.2 (2012), pp. 79–84.

- [2] Maristela L C et al. "Tumor islands in resected early-stage lung adenocarcinomas are associated with unique clinicopathologic and molecular characteristics and worse prognosis." In: *The American journal of surgical pathology* 37.2 (2013), pp. 287–94.
- [3] S Ourselin et al. "Reconstructing a 3D structure from serial histological sections". In: *Image and Vision Computing* 19.2000 (2001), pp. 25–31.
- [4] J Modersitzki et al. "Registration of histological serial sectionings". In: *Mathematical Models for Registration and Applications to Medical Imaging* (2006), pp. 63–80.
- [5] Marco Feuerstein et al. "Reconstruction of 3-D histology images by simultaneous deformable registration." In: *MICCAI - International Conference on Medical Image Computing and Computer-Assisted Intervention, LNCS 6892*. Ed. by G. Fichtinger et al. Vol. 14. Pt 2. Springer, 2011, pp. 582–589.
- [6] Yi Song et al. "3D reconstruction of multiple stained histology images". In: *Journal of Pathology Informatics* 4.2 (2013), p. 7.
- [7] Nicholas Roberts et al. "Toward routine use of 3D histopathology as a research tool." In: *The American journal of pathology* 180.5 (2012), pp. 1835–42.
- [8] Albert Cardona et al. "An integrated micro- and macroarchitectural analysis of the Drosophila brain by computer-assisted serial section electron microscopy." In: *PLoS biology* 8.10 (2010).
- [9] Kun Huang et al. "Fast automatic registration algorithm for large microscopy images". In: *Life Science Systems and Applications Workshop*. 1. IEEE/NLM, 2006, pp. 1–2.
- [10] N. Papenberg et al. "Registrierung im Fokus". In: *Bildverarbeitung für die Medizin* (2008), pp. 138–142.
- [11] Eldad Haber et al. "Intensity gradient based registration and fusion of multi-modal images." In: *Methods of Information in Medicine*. Lecture Notes in Computer Science 46.3 (2006). Ed. by Rasmus Larsen et al., pp. 292–299.
- [12] Jan Modersitzki. *FAIR: Flexible Algorithms for Image Registration*. SIAM, 2009.
- [13] B Mueller et al. "3D reconstruction of lung adenocarcinomas—one module for the development of mathematical multiscale models of lung cancer". In: *Abstracts of the 97th Annual Meeting of the German Society of Pathology. May 23-26, 2013. Heidelberg. Germany. Der Pathologe* 34 Suppl 1.1 (2013), p. 135.
- [14] D P Huttenlocher et al. "Comparing images using the Hausdorff distance". In: *Pattern Analysis and Machine Intelligence, IEEE Transactions on* 15.9 (1993), pp. 850–863.
- [15] LR Dice. "Measures of the amount of ecologic association between species". In: *Ecology* 26.3 (1945), pp. 297–302.

**This work is not being and has not been submitted for publication or presentation elsewhere.**